

such as those discussed in this paper for the following reasons. A biphotonic or bimolecular process such as process 4 is of course more probable if a high local concentration of excited states is produced, which is usually the case within the first millimeter of a highly concentrated complex solution absorbing the light. This is exactly the situation encountered in PEC since the illumination through the SnO₂ electrode generates the highest concentration of transient electroactive species at the electrode where the detection is carried out. It is also the case when the luminescence, for concentrated solutions, is measured as in the method of diffuse reflectance, i.e., from the same side as the excitation. In contrast, the spectroscopic detection of absorbing transients perpendicularly to the exciting beam is of course much less appropriate for such highly concentrated solutions.

Interestingly this PEC study has also shown that the stability of the oxidized complexes (Ru³⁺) in water decreases with the number of tap ligands: Ru(bpy)₃³⁺ and Ru(bpy)₂(tap)³⁺ behave

as stable species in the investigated time domain of PEC, whereas Ru(tap)₃³⁺ and, to a lesser extent, Ru(tap)₂(bpy)³⁺ are too unstable to be detected by PEC.

A last positive aspect of this PEC study is evidenced by the analysis of ΔV as a function of time, which may lead to the lifetime of the transient electroactive species in the presence and in the absence of oxygen. Thus, the Ru(tap)₃¹⁺ species in deoxygenated water has a lifetime limited to 57 ms, whereas in deoxygenated acetonitrile it is quite stable.

Acknowledgment. K. K. thanks the IRSIA (Institut pour la Recherche Scientifique dans l'Industrie et l'Agriculture) for a fellowship.

Registry No. SnO₂, 18282-10-5; LiNO₃, 7790-69-4; (Bu-t)₄NPF₆, 3109-63-5; CH₃CN, 75-05-8; Ru(bpy)₃²⁺, 15158-62-0; Ru(bpy)₂(tap)²⁺, 117183-30-9; Ru(bpy)(tap)₂²⁺, 117183-28-5; Ru(tap)₃²⁺, 88181-60-6; O₂, 7782-44-7; S₂O₈²⁻, 15092-81-6.

Kinetics of the Reactions of Partially Halogenated Methyl Radicals (CH₂Cl, CH₂Br, CH₂I, and CHCl₂) with Molecular Chlorine

J. A. Seetula, D. Gutman,*

Department of Chemistry, Catholic University of America, Washington D.C. 20064

P. D. Lightfoot,*

Laboratoire de Photophysique et Photochimie Moléculaire URA 348-CNRS, Université de Bordeaux I, 33405 Talence Cedex, France

M. T. Rayes,

Laboratoire de Physicochimie Théorique URA 503-CNRS, Université de Bordeaux I, 33405 Talence Cedex, France

and S. M. Senkan

Department of Chemical Engineering, University of California, Los Angeles, California 90024

(Received: April 24, 1991)

The gas-phase kinetics of the reactions of four partially halogenated methyl radicals (CH₂Cl, CH₂Br, CH₂I, and CHCl₂) with Cl₂ have been studied as a function of temperature using a tubular reactor coupled to a photoionization mass spectrometer. Radicals were homogeneously generated by pulsed 193- and/or 248-nm laser photolysis. Decays of the radical concentrations were monitored in time-resolved experiments as a function of [Cl₂] to obtain bimolecular rate constants for the R + Cl₂ → RCl + Cl reactions studied. The following Arrhenius expressions ($k = A \exp(-E/RT)$) were obtained (the numbers in brackets are log (A/(cm³ molecule⁻¹ s⁻¹)), E/(kJ mol⁻¹); the temperature ranges are also indicated): R = CH₂Cl [-11.82 ± 0.12, 4.1 ± 1.3, 295-719 K]; R = CH₂Br [-11.91 ± 0.14, 2.4 ± 1.4, 295-524 K]; R = CH₂I [-11.94 ± 0.19, 0.8 ± 2.2, 295-524 K]; R = CHCl₂ [-12.07 ± 0.15, 10.3 ± 2.0, 357-719 K]. Errors are 1σ, including both random and an estimated 20% systematic error in the individual bimolecular rate constants. The Arrhenius parameters of these and two other R + Cl₂ reactions are compared with theoretical determinations based on semiempirical AM1 calculations of transition-state energies, structures, and vibration frequencies. The calculations qualitatively reproduce the observed trends in both the Arrhenius A factors and in the activation energies. The use of molecular properties to account for reactivity differences among all the R + Cl₂ reactions which have been studied to date are also explored using free-energy correlations with these properties.

Introduction

Recent interest in the combustion,¹ atmospheric oxidation,² and oxidative pyrolysis³ of halogenated hydrocarbons has given rise to a need for kinetic data on the elementary reactions of halogenated carbon-based radicals in order to improve our understanding of these complex processes. The kinetic data base for such radicals is much less extensive than that for nonsubstituted hydrocarbon radicals, particularly at the elevated temperatures

pertaining to combustion processes.

As part of our program of study of the reactions of polyatomic carbon-based free radicals with a number of halogen-containing diatomic molecules,⁴⁻⁹ we have previously studied the reactions

(4) Timonen, R. S.; Gutman, D. *J. Phys. Chem.* **1986**, *90*, 2987.

(5) Timonen, R. S.; Russell, J. J.; Sarzynski, D.; Gutman, D. *J. Phys. Chem.* **1987**, *91*, 1873.

(6) Timonen, R. S.; Russell, J. J.; Gutman, D. *Int. J. Chem. Kinet.* **1986**, *18*, 1193.

(7) Timonen, R. S.; Seetula, J. A.; Niiranen, J.; Gutman, D. *J. Phys. Chem.* **1991**, *95*, 4009.

(8) Seetula, J. A.; Russell, J. J.; Gutman, D. *J. Am. Chem. Soc.* **1990**, *112*, 1347.

(9) Seetula, J. A.; Gutman, D. *J. Phys. Chem.* **1991**, *95*, 3626.

(1) Chang, W. D.; Senkan, S. M. *Environ. Sci. Technol.* **1989**, *23*, 442.

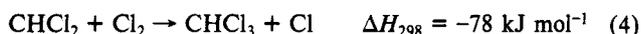
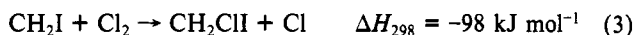
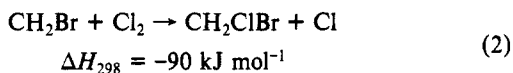
(2) World Meteorological Organization, Global Ozone Research and Monitoring Project, Report No. 16, Geneva, 1986.

(3) Senkan, S. M. *Chem. Eng. Prog.* **1987**, *12*, 58.

of Cl₂ with saturated hydrocarbon radicals,⁴ unsaturated hydrocarbon radicals,⁵ and perhalogenated methyl radicals.⁶ A wide range of reactivity, as manifested by differences in both the *A* factors and activation energies, was observed and found to be dependent on several factors, such as reaction exothermicity, radical ionization potential, and the presence of halogen atoms at the radical center.

No data exist on the corresponding reactions of partially halogenated alkyl radicals. There is a need for kinetic data on the reactions of these radicals with Cl₂ to interpret the experimental observations of other kinetic studies. For example, in a recent investigation of the temperature dependence of the CH₂Cl + CH₂Cl and CHCl₂ + CHCl₂ association reactions using the flash photolysis-UV absorption technique, Roussel et al.¹⁰ produced CH₂Cl and CHCl₂ by the flash photolysis of Cl₂ in the presence of CH₃Cl and CH₂Cl₂, respectively; rate constants for the reactions of these two radicals with Cl₂ were needed to assess the importance of chain processes in the overall reaction mechanism.

To broaden our understanding of the chemical kinetics of R + Cl₂ reactions and to address the above-mentioned need, we have now investigated the kinetics of the following reactions:¹¹



The reactions were isolated for quantitative study in a heatable tubular reactor coupled to a photoionization mass spectrometer. The free radicals of interest were generated by pulsed homogeneous excimer (ArF or KrF) photolysis of suitable precursors. The radical decays were monitored in time-resolved experiments. Arrhenius parameters for each rate constant were obtained from the results of experiments conducted at different temperatures. Direct observation of the halomethane product enabled the apparent mechanisms to be confirmed for reactions 1, 2, and 4. The results obtained are compared to previous results from this laboratory on other R + Cl₂ reactions and are interpreted with the aid of semiempirical quantum mechanical calculations. Finally, different free energy relationships are used to search for correlations between reactivity and reactant molecular properties among all the R + Cl₂ reactions that have been studied to date.

Experimental Section

The apparatus and its use for this kind of kinetic study have already been described in detail,^{4-9,19} and only a brief summary is given here. Pulsed, unfocused 193- or 248-nm radiation from

(10) Roussel, P.; Lightfoot, P. D.; Caralp, F.; Catoire, V.; Lesclaux, R. *11th International Symposium on Gas Kinetics*, Assisi, Italy, 2-7th Sept 1990. Roussel, P.; Lightfoot, P. D.; Caralp, F.; Catoire, V.; Lesclaux, R. *J. Phys. Chem.*, to be submitted.

(11) Heats of formation used to calculate heats of reaction were taken from the following: CH₃Cl, CH₂Cl₂, CHCl₃, Cl, ref 12; CH₂BrCl, ref 13; CH₃, ref 14; CH₂Cl, CHCl₂, CH₂Br, averages of the recommended values in refs 15 and 16; CH₂I, average of the recommended values in refs 16 and 17; CCl₃, ref 18; CH₂ICl, calculated for this study using the AM1 method. Calculated values of ΔH°_f for CH₂Cl₂ and CH₂ClBr were 13.0 and 10.5 kcal mol⁻¹ below the experimental values, respectively. Correcting the calculated result for CH₂ClI by the average of these two errors gives $\Delta H^\circ_f(\text{CH}_2\text{ClI}) = 10.5 \text{ kJ mol}^{-1}$.

(12) Chase Jr., M. W.; Davies, C. A.; Downey Jr., J. R.; Frurip, D. J.; McDonald, R. A.; Syverud, A. N. *J. Phys. Chem. Ref. Data* **1985**, *14*, Suppl. No. 1.

(13) Tschuikow-Roux, E.; Faraji, F.; Paddison, S.; Niedzielski, J.; Miyokawa, K. *J. Phys. Chem.* **1988**, *92*, 1488.

(14) Russell, J. J.; Seetula, J. A.; Senkan, S. M.; Gutman, D. *Int. J. Chem. Kinet.* **1988**, *20*, 759.

(15) Tschuikow-Roux, E.; Paddison, S. *Int. J. Chem. Kinet.* **1987**, *19*, 15.

(16) Holmes, J. L.; Lossing, F. P. *J. Am. Chem. Soc.* **1988**, *110*, 7343.

(17) Furuyama, S.; Golden, D. M.; Benson, S. W. *Int. J. Chem. Kinet.* **1969**, *1*, 283.

(18) Hudgens, J. W.; Johnson III, R. D.; Timonen, R. S.; Seetula, J. A.; Gutman, D. *J. Phys. Chem.* **1991**, *95*, 4400.

(19) Slagle, I. R.; Gutman, D. *J. Am. Chem. Soc.* **1985**, *107*, 5342.

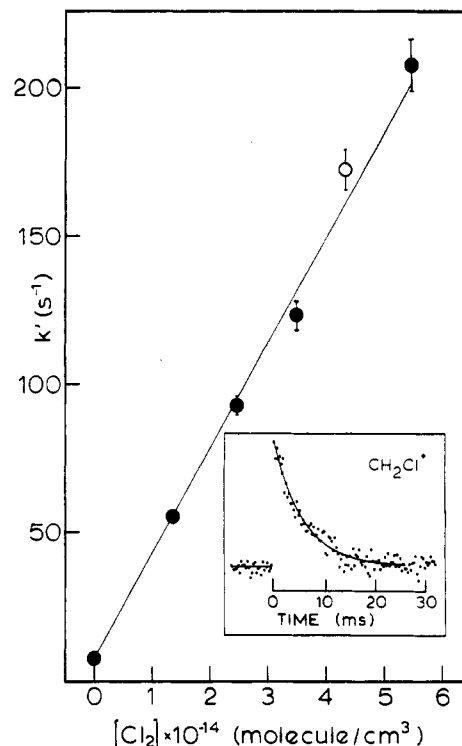
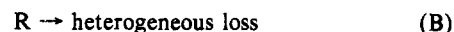
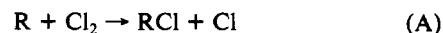


Figure 1. Plot of exponential decay constants of the CH₂Cl⁺ ion signals measured at 357 K and a total density of 5.81×10^{16} molecules cm⁻³ (see Table I for more details). Insert is the actual ion signal for the experiment corresponding to the unfilled circle, $[\text{Cl}_2] = 4.3 \times 10^{14}$ molecules cm⁻³. The line through the decay is an exponential function fitted by nonlinear least-squares techniques. The straight line corresponds to a weighted linear regression to the individual points. The first-order decay constant (*k'*) for CH₂Cl in the displayed ion signal profile is $173 \pm 7 \text{ s}^{-1}$.

a Lambda Physik EMG 201 MSC excimer laser, operating at 5 Hz, was collimated and then directed along the axis of a 1.05-cm-i.d. tubular reactor. Laser fluence was varied using quartz flats or wire screens placed between the laser and the reactor. Two reactors were used, one of quartz construction, uncoated, the other of Pyrex, coated with Teflon. Gas flowing through the tube at 5 m s^{-1} was completely replaced between laser pulses. The flowing gas contained the radical precursor in very low concentrations (typically 0.01%), Cl₂ in varying amounts (0.1–2.0%), and the He carrier gas in large excess (>98%). The precursors for CH₂Cl, CH₂Br, CH₂I, and CHCl₂ were CH₂ClBr (Aldrich, 99%), CH₂Br₂ (Aldrich, >99%), CH₂ClI (Aldrich, 97%), and CHCl₂Br (Aldrich, >98%), respectively. All precursors and Cl₂ (Matheson 99.9%) were degassed by freeze-pump-thaw cycles before use. Helium (Matheson, 99.995%) was used as supplied.

Gas was sampled through a 0.4-mm hole located at the apex of a cone-shaped orifice in the wall of the reactor and formed into a beam by a conical skimmer before it entered the vacuum chamber containing the photoionization mass spectrometer. As the beam traversed the ion source, a portion was photoionized using an atomic resonance lamp. Mass-selected ion signals were recorded from a short time before the laser pulse to up to 26 ms afterward, using a multichannel scalar. Data from 1000 to 15000 laser shots were accumulated in each experiment to obtain the quality of data sought.

Molecular chlorine was always in great excess over the initial radical concentration, resulting in pseudo-first-order kinetics. Only two processes were responsible for the loss of the free radical, R:



An exponential decay constant, *k'*, was obtained from each radical-decay profile using a nonlinear least-squares analysis program. Bimolecular rate constants for reactions 1–4 were obtained from the slopes of plots of *k'* against $[\text{Cl}_2]$. The linear regression fit

TABLE I: Conditions and Results of Experiments To Measure R + Cl₂ Rate Constants

T, K	10 ⁻¹⁶ [He], molecules cm ⁻³	10 ⁻¹⁴ [Cl ₂], molecules cm ⁻³	k _w , s ⁻¹	wall coating material ^b	10 ¹³ k, cm ³ molecule ⁻¹ s ⁻¹
CH ₂ Cl + Cl ₂ → CH ₂ Cl ₂ + Cl					
k ₁ = (1.5 ± 0.5) × 10 ⁻¹² exp((-4.1 ± 1.3) kJ mol ⁻¹ /RT) ^d cm ³ molecule ⁻¹ s ⁻¹					
295	5.80	1.28–5.88	16	T	3.10 ± 0.15
295	14.7	1.71–4.73	12	T	3.10 ± 0.23
324	5.79	1.07–6.21	11	T	3.13 ± 0.15
357	5.81	1.37–5.45	7.3	T	3.54 ± 0.20
358	5.83	1.43–4.51	19	Q	3.98 ± 0.18
400	5.85	1.32–5.67	12	T	4.07 ± 0.20
453	5.84	1.40–5.20	7.9	T	4.67 ± 0.15
458	5.79	1.59–4.02	14	Q	5.04 ± 0.27
524	5.85	1.67–5.61	7.3	T	5.28 ± 0.20
524 ^e	5.85	1.16–4.42	8.4	T	5.45 ± 0.26
533	5.75	0.67–4.13	19	Q	6.46 ± 0.48
615	5.72	0.83–3.84	25	Q	6.72 ± 0.63
719	5.72	0.54–2.63	12	Q	9.22 ± 0.54
CH ₂ Br + Cl ₂ → CH ₂ ClBr + Cl					
k ₂ = (1.2 ± 0.5) × 10 ⁻¹² exp((-2.4 ± 1.4) kJ mol ⁻¹ /RT) ^d cm ³ molecule ⁻¹ s ⁻¹					
295 ^e	5.68	1.17–4.35	10	T	4.59 ± 0.35
295 ^e	14.8	1.13–3.98	10	T	4.82 ± 0.25
324 ^e	5.79	1.28–3.74	16	T	5.13 ± 0.66
357 ^e	5.81	1.33–3.03	11	T	5.18 ± 0.47
400 ^e	5.83	1.14–4.46	12	T	6.03 ± 0.12
453 ^e	5.86	0.99–3.59	11	T	6.47 ± 0.41
524 ^e	5.87	0.82–3.07	16	T	7.26 ± 0.33
CH ₂ I + Cl ₂ → CH ₂ ClI + Cl					
k ₃ = (1.2 ± 0.6) × 10 ⁻¹² exp((-0.8 ± 2.2) kJ mol ⁻¹ /RT) ^d cm ³ molecule ⁻¹ s ⁻¹					
295	5.81	1.22–5.07	25	T	7.91 ± 0.72
358	5.83	0.50–3.19	41	Q	10.28 ± 1.90
458	5.78	0.70–3.42	53	Q	9.17 ± 1.31
524	5.87	0.65–4.63	53	T	9.41 ± 0.52
CHCl ₂ + Cl ₂ → CHCl ₃ + Cl					
k ₄ = (8.6 ± 3.6) × 10 ⁻¹³ exp((-10.3 ± 2.0) kJ mol ⁻¹ /RT) ^d cm ³ molecule ⁻¹ s ⁻¹					
357 ^e	14.8	11.1–21.4	6.4	T	0.287 ± 0.011
357 ^e	14.8	8.80–19.6	1.1	T	0.285 ± 0.038
400 ^e	14.8	6.88–22.9	7.7	T	0.362 ± 0.013
453 ^e	5.85	4.00–11.6	6.9	T	0.481 ± 0.031
453 ^e	14.8	6.53–17.9	3.6	T	0.514 ± 0.036
458 ^e	6.75	5.04–16.2	1.9	Q	0.635 ± 0.046
524 ^e	5.86	4.04–11.6	6.3	T	0.747 ± 0.020
533 ^e	5.74	3.71–13.1	8.2	Q	0.783 ± 0.039
615 ^e	5.72	2.09–12.5	4.1	Q	1.27 ± 0.15
719 ^e	5.86	1.93–11.8	3.0	Q	1.69 ± 0.27

^aTemperature uncertainties are ±2 K (295–400 K), ±3 K (453–533 K), ±7 K (615–719 K). ^bT: poly(tetrafluoroethylene)-coated Pyrex reactor; Q: uncoated quartz reactor. ^cErrors are 1σ and refer to statistical uncertainties only. ^dErrors are 1σ, which include estimated 20% upper limit to possible systematic errors. ^e248-nm photolysis; all other experiments used 193-nm photolysis.

was weighted by the statistical uncertainties associated with the measured values of k', and the uncertainties on the bimolecular rate constant calculated using the largest of the internal and external errors.²⁰ A typical ion signal decay profile and decay constant plot from one set of experiments to measure k₁ are shown in Figure 1.

Before each set of experiments, the wall loss rate constant was determined in the absence of Cl₂. The laser fluence was reduced until this effective wall loss rate constant and the rate constants in the presence of Cl₂ were independent of laser fluence. Under these conditions, it was presumed that radical-radical and radical-atom reactions were of negligible importance compared to the reaction of interest. Typical laser fluences were 110 mJ cm⁻²

TABLE II: Summary of Arrhenius Parameters and Thermochemistry for the Reactions of Polyatomic Free Radicals (R) with Molecular Chlorine

R	IP of R, ^a eV	ΔH, ^b kJ mol ⁻¹	log (A/cm ³ molecule ⁻¹ s ⁻¹) ^c	E _a , ^c kJ mol ⁻¹	ref ^d
i-C ₄ H ₉	6.6	-108	-10.40 ± 0.26	0 ± 2	5
i-C ₃ H ₇	7.4	-112	-10.60 ± 0.26	-2 ± 3	5
C ₂ H ₅	8.4	-110	-10.90 ± 0.33	-1 ± 3	5
CH ₃	9.8	-108	-11.27 ± 0.09	3 ± 1	5
CH ₂ Cl	8.8	-93	-11.82 ± 0.12	4 ± 1	cs
CHCl ₂	8.3	-78	-12.07 ± 0.15	10 ± 2	cs
CCl ₃	8.3	-49	(-12.17)	(21)	5
CH ₂ Br	8.6	-90	-11.91 ± 0.14	2 ± 1	cs
CH ₂ I	n/a	-98	-11.94 ± 0.19	1 ± 2	cs
C ₂ H ₃	8.7	-147	-11.06 ± 0.35	-2 ± 5	5
C ₃ H ₃	8.7	-62	-10.56 ± 0.35	28 ± 5	5
C ₃ H ₅	8.1	-49	-10.81 ± 0.26	18 ± 3	5
HCO	8.6	-85	-11.16 ± 0.24	0 ± 2	5
CF ₃	9.5	-117	-11.35 ± 0.35	15 ± 5	5
CF ₂ Cl	8.4	-103	-11.89 ± 0.24	8 ± 3	5
CFCl ₂	8.1	-68	-11.86 ± 0.31	14 ± 4	5

^aIonization potentials of free radicals from ref 23. ^bReaction enthalpies at 300 K. Origins of heats of formation used to calculate ΔH in cited references. For reactions in the current study, see ref 9. ^cQuoted errors are 1σ. Arrhenius parameters and errors were calculated from the fits weighted by the experimental uncertainty in the bimolecular rate constant at each temperature. ^dcs indicates current study.

at 193 nm and 45 mJ cm⁻² at 248 nm. Calculations based on the measured percentage photolysis of the precursor molecules suggest initial radical densities of the order (1–8) × 10¹⁰ radicals cm⁻³.

The possibility of a significant bimolecular heterogeneous reaction occurring between the same reactants (R + Cl₂) in these experiments was excluded based on the results of experiments conducted using both the uncoated quartz and coated Pyrex reactor (coated with Teflon). The measured rate constants of reactions 1–4 were independent of the reactor wall surface material. Since the two wall materials have quite different adsorption characteristics, we conclude that these results prove that bimolecular heterogeneous R + Cl₂ reactions, if they occurred at all, were of no significance in these experiments.

Excimer photolysis of the precursor molecules produces vibrationally excited radicals, but it is expected that the radicals are thermalized quickly before there is noticeable reaction (on a submillisecond time scale in these experiments^{21,22}). The vibrational relaxation time of the radicals was shortened by conducting experiments at a bath gas density that was higher by over a factor of 2. There was no noticeable difference between the rate constants obtained at different densities, demonstrating that the radicals were indeed thermalized in a time short compared to the observation time of the radical decays (typically 10–25 ms).

The photoionization energies used in the mass spectrometer to detect reactants and products were as follows: 8.9–9.1 eV for the radicals, 10.2 eV for CH₂ClI, and 11.6–11.8 eV for CH₂Cl₂, CHCl₃, CH₂ClBr, and CH₂Br₂.

For reactions 1, 2, and 4, the production of the halomethane product could be observed. For reaction 2, the rate constant for the exponential growth of CH₂ClBr matched that of the decay of CH₂Br closely; for reactions 1 and 4, poor signal-to-noise caused by a high background precluded precise determination of the rate constant for product buildup, but in each case it was compatible with that of the corresponding radical decay. For reaction 3, it was not possible to monitor the buildup of the product as it was the same molecule as the precursor.

The bimolecular rate constants obtained for reactions 1–4 and the experimental conditions used for their measurement are listed in Table I. The rate constants for each reaction were fitted to the Arrhenius expression, each point being weighted by its ex-

(21) Donaldson, D. J.; Leone, S. R. *J. Phys. Chem.* **1987**, *91*, 3128.(22) Young, M. A.; Pimentel, G. C. *J. Phys. Chem.* **1990**, *94*, 4884.(20) Cvetanovic, R. J.; Singleton, D. L.; Paraskevopoulos, G. *J. Phys. Chem.* **1979**, *83*, 50.(23) Lias, S. G.; Bartmess, J. E.; Liebman, J. F.; Holmes, J. L.; Levin, R. D.; Mallard, W. G. *J. Phys. Chem. Ref. Data* **1988**, *17*, 1.

TABLE III: Summary of Calculated Transition-State Parameters

R	r(C-Cl), Å	r(Cl-Cl), Å	angle C-Cl-Cl, deg
CH ₃	2.23	1.938	147.8
CH ₂ Cl	2.11	1.945	142.6
CHCl ₂	2.00	1.953	137.9
CCl ₃	1.90	1.960	131.3
ClCl ^a		1.917	

^aCl₂ included in table to display equilibrium Cl-Cl bond distance.

TABLE IV: Comparison of Calculated and Experimental Arrhenius Parameters

R	E _a , kJ mol ⁻¹		A, cm ³ molecule ⁻¹ s ⁻¹	
	exp	AM1	exp	AM1
CH ₃	2	6	4.8 (-12)	6.1 (-12)
CH ₂ Cl	4.1	20	1.5 (-12)	2.0 (-12)
CHCl ₂	10.1	39	8.6 (-13)	4.2 (-13)
CH ₂ Br	2.4	20	1.2 (-12)	6.4 (-13)
CH ₂ I	0.8	19	1.2 (-12)	6.8 (-13)
CCl ₃	(21)	60	(6.8 (-13))	a

^aThe transition state was not sufficiently well localized in the case of CCl₃ to calculate the A factor.

perimental uncertainty, plus an estimated 20% upper limit systematic error. Arrhenius plots of the rate constants are shown in Figure 2. The Arrhenius parameters of these four reactions are given in Table II together with those of other R + Cl₂ reactions that were obtained earlier.⁴⁻⁶

Calculations

To gain some insight into the factors responsible for the differences in the rate constants for reactions 1-4, semiempirical molecular orbital calculations were performed not only on reactions 1-4 but also on the reactions of CH₃ and CCl₃ with Cl₂ using the AM1 method.²⁴ Reaction paths were determined at the UHF level. In each case, a saddle point was found on the route from reactants to products by searching for the configuration which was characterized by only one negative value of the second derivative of the potential energy surface; the transition state was assumed to be located at that point.

The geometries and vibration frequencies of the transition states were used to obtain the entropy and energy of activation as well as rate constant parameters which were fit to Arrhenius expressions. The most important results obtained are given in Tables III and IV. Table III shows three important geometrical properties of the transition states of the reactions of the chloromethyl + Cl₂ reactions: the C-Cl and Cl-Cl bond lengths, and the C-Cl-Cl bond angles.

In each of the R + Cl₂ reactions, the Cl-Cl bond length is close to that calculated for the free Cl₂ molecule. All the transition states are more reactant- than product-like. On going from CH₃ to CCl₃, the transition state C-Cl distance decreases and the Cl-Cl distance increases, resulting in a "tighter" transition state, presumably owing to a weakening of the C-Cl bond formed. This tendency results in a systematic decrease in the calculated A factors and an increase in the activation energies for the R + Cl₂ reactions with increasing Cl substitution in the methyl radical. These trends in the rate constant parameters can be seen in Table IV.

The calculated A factors are generally within a factor of 2 of the measured values and reproduce the experimental trend CH₃ > CH₂Cl > CH₂Br ≈ CH₂I > CHCl₂. The calculated activation energies are significantly greater than the experimental values, a situation commonly found when using semiempirical methods. However, the ordering of the calculated activation energies is in accord with the experimental values (CCl₃ > CHCl₂ > CH₂Cl, CH₂Br, CH₂I, CH₃).

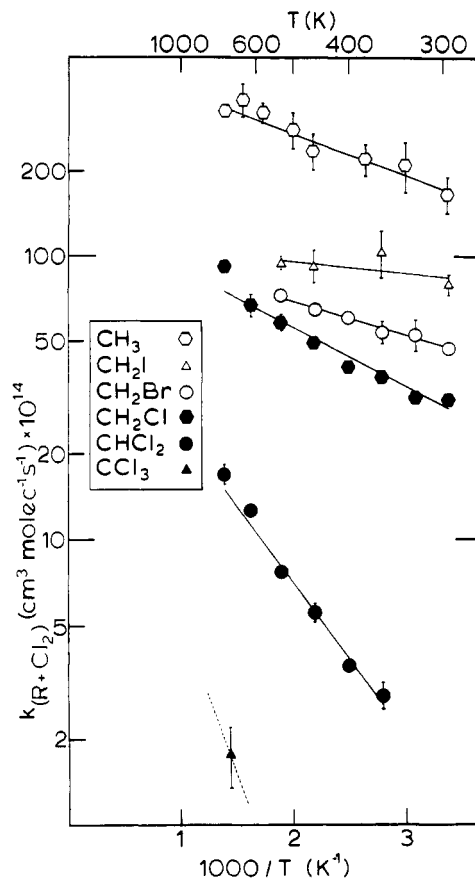


Figure 2. Arrhenius plot of measured R + Cl₂ rate constants obtained in the current study plus those for CH₃ + Cl₂⁴ and CCl₃ + Cl₂⁶ reactions.

Discussion

There now exists a significant body of information on the kinetics of reactions of polyatomic free radicals with Cl₂ (see Table II). A wide range of activation energies and A factors have been reported for these exothermic, apparently simple chlorine atom transfer reactions. In general, electron-withdrawing groups attached to the radical center decrease the rate constant for the reaction by both increasing the activation energy and reducing the A factor, as observed experimentally and as reproduced by the semiempirical calculations described above. Electron-donating groups have the opposite effect. As reported previously, these observations are consistent with a polar transition state in which there is some charge transfer from the radical to the chlorine molecule.⁵

To account for reactivity differences in terms of reaction or molecular properties, we have also searched for linear free energy relationships with different properties. The relationships with three different reaction variables used for this purpose were inspected: reaction enthalpy, radical ionization potential minus electron affinity of the second reactant (Cl₂ in this case), and a new scale, the Thomas-Seetula electronegativity difference scale (TSED, see below). log k_{300K} was used as the measure of the free energy of activation at a common temperature. (It would be more correct to use the corresponding reactive cross sections,²⁵ in order to eliminate reduced mass factors, but such factors are small compared with the large variation in the rate constants. We prefer to continue with the more common practice of using k_{300K}.)

Unfortunately, not all of the molecular properties needed for these free energy plots are available for all of the R + Cl₂ reactions studied. So the three plots do display information for different subsets of the group of R + Cl₂ reactions for which there is kinetic information. All the reaction enthalpies could be determined (16), 15 ionization potentials of radicals (for the IP-EA parameter) were available, but only 12 electronegativity factors could be calculated.

(24) Dewar, M. J. S.; Zoebisch, E. G.; Healy, E. F.; Stewart, J. J. P. *J. Am. Chem. Soc.* **1985**, *107*, 3902. Dewar, M. S. J.; Zoebisch, E. G. *J. Mol. Struct. (THEOCHEM)* **1988**, *180*, 1.

(25) Fenter, F. F.; Anderson, J. G. *J. Phys. Chem.* **1991**, *95*, 3172.

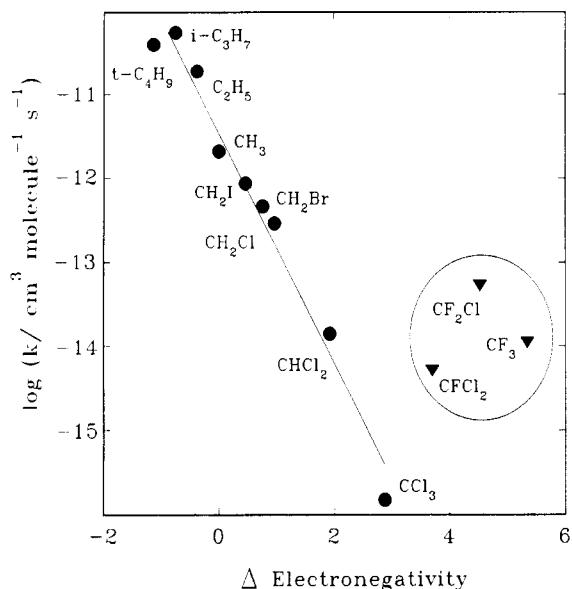


Figure 3. Free energy plot of $\log(k_{300K})$ vs the Δ electronegativity parameter (see text) for $R + Cl_2$ reactions involving substituted methyl radicals. The straight line represents a fit to all data, apart from those concerning fluorine-containing radicals (circled). Closed triangles represent points for radicals containing fluorine atoms at the radical center. Closed circles indicate all other radicals considered for which the Δ electronegativity parameter could be calculated.

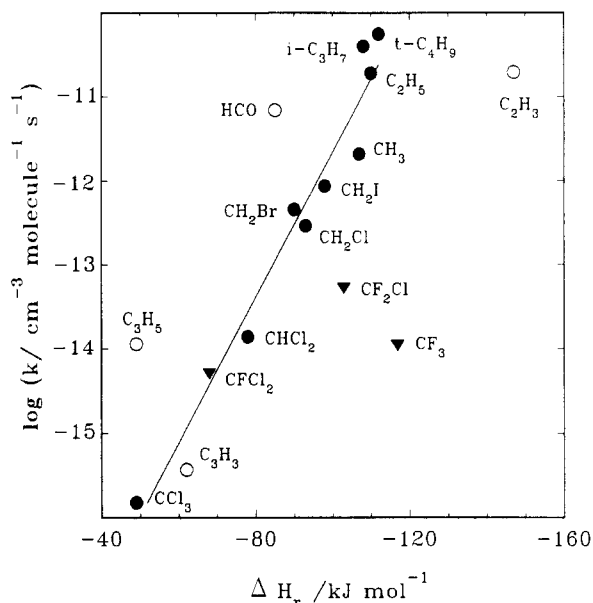


Figure 4. Free energy plot of $\log(k_{300K})$ vs the enthalpy of reaction for all $R + Cl_2$ reactions studied to date. Filled symbols represent those rate constants which are also plotted in Figure 3 (again closed triangles are used if the radical contains fluorine as a substituent and closed circles if fluorine is absent). The open circles indicate additional $R + Cl_2$ rate constants not plotted in Figure 3 (because the TSED parameter is not defined for these radicals).

The three free energy plots involving these variables are shown in Figures 3–5. To provide a common set of data on the three plots which can be used for comparison purposes, those points for the 12 reactions displayed on all three plots are indicated by solid circles. The remainder are displayed as open circles.

The TSED parameter, which was first developed by Thomas²⁶ for indicating the effect of electron-withdrawing groups on core electron energies, was more recently used in this laboratory as an indicator of the influence of electron-donating or electron-withdrawing groups on reactivity, specifically among the reactions

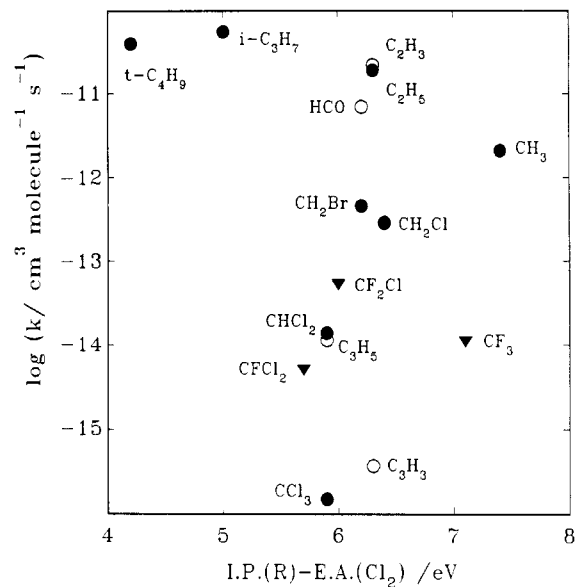


Figure 5. Free energy plot of $\log(k_{300K})$ vs $IP - EA$ for $R + Cl_2$ reactions. The symbols have the same meaning as in Figure 4. CH_2I is not included, as its ionization potential is not known.

of substituted methyl radicals with HI^9 and Br_2^7 . The TSED parameter (denoted Δ electronegativity in eq 5) is the algebraic

$$\Delta \text{electronegativity} = \sum_{i=1}^3 (X_i - X_H) \quad (5)$$

sum of the difference in the Pauling electronegativity of each of the three substituents (X_i) and that of H, the reference substituent (X_H).

An effective Pauling electronegativity of 1.82 for the CH_3 group was introduced by Seetula and Gutman⁹ to best linearize the free energy plot for reactions of alkyl radicals with HI^9 . The same effective CH_3 electronegativity provided a comparable linear relationship with the TSED parameter for the reactions of substituted methyl radicals with Br_2^7 .

It is seen in Figure 3 that for the common set of reactions, apart from those involving the fluorine-containing radicals (the circled data points in Figure 3), a linear free energy relationship exists with the TSED parameter for $R + Cl_2$ reactions, one which spans nearly 6 orders of magnitude in the room-temperature rate constant. The same anomalous behavior observed here for the reactions of the fluorine-containing radicals CF_3 , CF_2Cl , and $CFC1_2$ was also observed for the reactions of these same radicals with Br_2^7 . The rate constants for these latter radicals with both Cl_2 and Br_2 can be made to comply with the linear relationship displayed in Figure 3 by introducing another adjustable parameter, the "effective" electronegativity of fluorine, assigning it a value of 2.8, which is significantly lower than the value based on the Pauling value for an isolated fluorine atom, 3.98.²⁷ The small size of the fluorine atom has been previously cited as partially responsible for the fact that its ability to accept negative charge in bonding situations ("effective" electronegativity) is anomalously low when compared to its "intrinsic", i.e., Pauling, electronegativity.²⁷

The free energy correlation with reaction enthalpy is shown in Figure 4 where values of $\log k_{300K}$ are plotted against $\Delta H_{r,300K}$. While a general trend of increasing reactivity with increasing exothermicity is apparent, the trend is not systematic and is not linear. However, a roughly linear relationship does exist for the subset of common reactions (particularly when the points representing the reactions of the fluorine-containing radicals are again excluded).

Finally, in Figure 5 a plot of $\log(k_{300K})$ vs $(IP(R) - EA(Cl_2))$ is displayed. Similar $(IP - EA)$ plots have been found to provide

(26) Thomas, T. D. *J. Am. Chem. Soc.* **1970**, *92*, 4184.

(27) Huheey, J. E. *Inorganic Chemistry*; Harper & Row: New York, 1972; Chapter 4, p 160.

good correlations for the reactions of a number of free radicals with O₃,²⁸ O₂,²⁹ and NOCl,³⁰ the rate constant increasing with a decreasing difference between IP and EA. Such behavior is thought to be indicative of interaction with low-lying ionic states which can lower the barrier to reaction or increase the *A* factor by stabilizing the partial charge transfer in the transition state.²⁸ It was previously observed that there is a good linear correlation between log(*k*_{300K}) and (IP(R) - EA(Cl₂)) when R is the set of alkyl radicals.⁴ However, Figure 5 shows clearly that the correlation between rate constant and IP - EA indicated for the alkyl radicals has no resemblance to that displayed by the R + Cl₂ rate constants when halogen atoms are attached to the radical site. For these latter reactions, even the direction of the trend in rate constants with this parameter is reversed, lower IP - EA differences are generally associated with the lower rate constants.

In a recent refinement of the use of this last parameter for use in free energy plots, Fenter and Anderson²⁵ have modified the (IP - EA) correlation to take into account the effect of the polarizabilities (α) of the two reactants. Plots of log(*k*_{300K}) against (IP - EA)/($\alpha_1 + \alpha_2$), i.e., the lowest of the two possible values of (IP - EA) divided by the sum of the polarizabilities of the two reactants, were found to give a much better correlation for the reactions of OH, O, S, and SD with a number of halogen molecules, including Cl₂, than a simple (IP - EA) plot. The greater polarizability of Br₂ over Cl₂ was also invoked to explain its greater reactivity towards a number of carbon-based free radicals.⁷

This modified IP - EA parameter was tested to determine whether it provides a more useful free energy relationship, i.e., one capable of accounting for reactivity trends among R + Cl₂ reactions involving both halogenated and nonhalogenated radicals. Average polarizabilities for CH₃, CH₂Cl, CHCl₂, and CCl₃ were calculated using the PM3 method,³¹ resulting in values of 0.85, 1.96, 3.37, and 4.94 Å³, respectively. While a linear relationship does exist between log(*k*_{300K}) and (IP(R) - EA(Cl₂))/($\alpha_1 + \alpha_2$) for the series of reactions, CH₃...CCl₃ + Cl₂, the trend is still opposite in direction to that displayed by the alkyl radical + Cl₂ rate constants.

Conclusion

We summarize here the observations of reactivity vs reaction properties as displayed on the free energy plots displayed in Figures 3-5.

(28) Ruiz, R. P.; Bayes, K. D. *J. Phys. Chem.* **1984**, *88*, 2592.

(29) Paltenghi, R.; Ogryzlo, E. A.; Bayes, K. D. *J. Phys. Chem.* **1984**, *88*, 2595.

(30) Abbatt, J. P. D.; Toohey, D. W.; Fenter, F. F.; Stevens, P. S.; Brune, Wm. H.; Anderson, J. G. *J. Phys. Chem.* **1989**, *93*, 1022.

(31) Stewart, J. J. P. *J. Comput. Chem.* **1989**, *10*, 209.

(i) None of the three parameters used provides a comprehensive indication of the trends in reactivity among the R + Cl₂ reactions studied to date. Each parameter is particularly unsuitable for accounting for reactivity changes caused by fluorine substitution at the radical site.

(ii) The ionization potential of the free radical is a poor parameter to use to account for reactivity particularly when attempting to coalesce reactivity trends of halogen-substituted radicals and non-halogen-substituted radicals.

(iii) There is a qualitative indication that reaction enthalpy is an important factor in determining reaction rate constants, but clearly other factors are also rate determining. This free energy relationship is roughly linear for the set of reactions involving substituted methyl radicals (again excluding the fluorine-substituted radicals). However, serious deviations are apparent for other radicals, e.g., unsaturated C₂ and C₃ radicals and HCO.

(iv) The TSED scale developed in this laboratory for accounting for reactivity differences among the free radical reactions with HI and Br₂ also is suitable in the case of the reactions with Cl₂, apart from the fluorine-containing radicals (although, as stated above, reasonable agreement can be obtained for these radicals as well if an effective electronegativity of 2.8 is assigned to F). Electron-withdrawing groups both increase the activation energy and reduce the *A* factor for the reaction, in good agreement with the results of the present AM1 calculations, which indicate a tightening of the transition state with increasingly electronegative substituents.

The presence of electron-donating groups results in near-zero activation energies in the R + Cl₂, HI, and HBr reactions. It is interesting to note that the TSED scale is successful in correlating both those reactions which have no apparent activation energy and those reactions which have significant activation energies, whereas the enthalpy of reaction scale and the ionization potential scale only provide near linear correlations for either the reactions with or the reactions without activation energies taken separately. It would appear that, for reactions without barriers, which are essentially entropy-controlled, the TSED parameter, like the (IP - EA) parameter, provides a good indicator of the importance of long-range interactions.

Acknowledgment. Support for this research was provided by the National Science Foundation, Division of Chemical, Biochemical and Thermal Engineering, under Grant CTS-98191704. We thank Dr. Irene R. Slagle for her advice, help, and assistance. J.A.S. thanks the Natural Science Council of the Academy of Finland and the Finnish Cultural Foundation for fellowships. We also thank Dr. F. Fenter for a prepublication copy of ref 25.

Registry No. CH₂Cl, 6806-86-6; CH₂Br, 16519-97-4; CH₂I, 16519-98-5; CHCl₂, 3474-12-2; Cl₂, 7782-50-5.